2006 AMOS Technical Conference

Integrated Multi-Sensor System for Enhanced Space Surveillance – Design, Engineering, Integration and Tests

Shiang Liu
The Aerospace Corporation, 2350 El Segundo Bl.,El Segundo, CA, 90245

Vladimir B. Markov, Anatoliy Khizhnyak
MetroLaser Inc., 2572 White Rd., Irvine, CA, 92614-6236

Roberta Ewart
AF Space and Missile Systems Center, LAAFB, CA 90245

Doug Craig
Air Force Research Laboratory, Space Vehicle Directorate, AFB, NM 87117-5776

ABSTRACT

Space surveillance requires capabilities for detection, tracking, imaging and characterization of specific objects in space environment. In general, most current space surveillance systems are single-sensor based and are not capable of generating the desired tracking accuracy, and providing required object characterization. A suite of various types of the sensors that are spatially or temporarily separated may thus be used collectively to synthesize a composite, improved surveillance picture through fusion and post processing of retrieved data. However, this approach will not yield the highest possible data accuracy due to the errors introduced in correlation of location, orientation and detection time from different sensors. Furthermore, it may not provide timely surveillance data to the user and hence may degrade the utility of these data. In this paper, we present the architecture, operational concept and preliminary design of an advanced integrated multi-sensor system (AIMS) for enhanced space surveillance capability to alleviate these shortfalls. AIMS employs an active laser tracking and multiple spectral domain (visible and multi-band IR) sensing to provide high-resolution tracking, three-dimensional imaging and reliable characterization of space objects with down range resolution of 1 cm and velocity measurement accuracy of 1-10 cm/sec in near real-time. The engineering and integration of a scale-down prototype of AIMS together with results of initial field tests are reported in this paper. Issues, lessons learned, future development plan and potential application of AIMS to space missions will be discussed.

1. INTRODUCTION

Improved capabilities in detecting, tracking, imaging and characterization of space objects are needed for space superiority mission. Majority of existing space surveillance systems are single-sensor based and are not capable of providing a comprehensive set of surveillance measures for accurate target characterization. For example, the effectiveness of passive space objects imaging sensors depends on sun illumination, thus leaving the Earth eclipsed targets less detectable. The fusion of data from multiple single-sensor based surveillance systems at different locations may encounter difficulty of superposing target features accurately. Post processing of time and space partitioned data sources with uncertainty in data delay may render outcome obsolete. This paper discusses the progress in development of an advanced integrated multi-sensor system (AIMS) for enhanced space surveillance capabilities to alleviate these deficiencies.

To achieve a responsive and enhanced surveillance performance, the AIMS employs a suite of sensors with their response across a broad spectral range through a shared optical train. It integrates an active laser tracking system (ALTS) module [1, 2, 3], visible and multi-band IR sensors (Near-IR, MWIR and LWIR) to provide a rich set of simultaneous surveillance measures that will enable high-resolution tracking/imaging and robust characterization of space targets. AIMS operations are performed using a common optical train, and should result in increased data reliability and near real-time target characterization with minimal data latency.

This paper summarizes the analysis, design, engineering and integration of an AIMS prototype. Preliminary results of limited laboratory and field testing are reported. Potential applications of AIMS to support space superiority and

other mission areas are also discussed.

2. ARCHITECTURE, DESIGN AND CONCEPT OF OPERATIONS

Existing approaches to track, point and discriminate (TPD) space objects involve a complex suite of interacting systems based on such technologies as radar, passive optical [4] and infrared sensing [5], photogrametry [6], polarimetry [7], multi-spectral imaging [8], and passive laser tracking [9]. However, current space surveillance capabilities are insufficient to meet the desired needs, such as detection and tracking of small/dim objects, event and threat detection and characterization, high-resolution 3D space object imagery, and on-demand target information gathering with minimum data latency. This insufficiency comes mostly as a result of the immense technical challenges involved, including great distances to target and optical aberrations along an observation path, needed hemispherical coverage and rapid search, responsive operation, and data fusion from multiple and nonidentical sensors. Laser-based methods allow to address some of these technical challenges, particularly effects of atmospheric turbulence along an aiming direction, high relative velocity between the surveillance platform and remote target, its vibrational spectrum, etc.

The proposed concept of the AIMS was suggested to address and improve certain issues of space surveillance. By integrating on a single platform and advanced coherent sensor module (ALTS) with emerging sophisticated visible and IR search and track (IRST) technologies this concept introduces an innovative approach to the problem of an integrated multi-sensor system for space surveillance. When fully developed and implemented it should enable detection, tracking, characterization, discrimination the space objects, as well as event identification, thus significantly enhancing the synergy of individual imaging systems. The initial state vector and cueing information for AIMS can be provided by conventional radars. Because AIMS will use an active imaging technology, it can operate in both day and night and for "dark pass" tracking of satellites through the Earth's -eclipsed zone. Additionally, active illumination provides a means for optical signal gating, which can greatly enhance the signal-to-noise ratio in an acquired image. Imaging data that includes multi-spectral information can be used for identifying the composition of the targets what is of great utility for discrimination purposes [10]. Based on the conceptual design of AIMS, an integrated system with a single illumination source could provide the same functionality as a collection of the detached and distributed sensors.

Another advantage of having sensors suite on a single platform with controlled active illumination is to facilitate data fusion, a major thrust in surveillance applications that has received much attention in recent years [11,12]. Active illumination allows accurate synchronization of several data streams, and a shared optical train ensures that the data is referenced to a common coordinate system and clock. As an added advantage, an integrated system can reduce the number of required target acquisition handoffs, an error-prone process that tends to slow the response of the tracking system in time-critical applications [13]. Since the proposed concept is a single platform, multiple sensor system that allows for multi-functional operations (target identification and characterization, plus event and threat detection), it is mandatory to miniaturize the complete system to enable space deployment.

Current AIMS architecture comprises of several sensors (ALTS, visible and IR) assembled on a single platform, as shown schematically in Fig. 1. In the prototype design, the AIMS can operate independently, although in perspective it can work cooperatively, grouping with other "external" systems, such as a large optical telescope, RF radar system, or a supercomputer for multi-platform data fusion. In the AIMS conceptual design, the laser ALTS module is the heart of the AIMS, allowing it to retrieve key features of the target, such as the 9D state vector (spatial coordinates R{x, y, z}, velocity R′, and acceleration R′′) and the spectrum of its mechanical vibrations. Integration of the IR and visible imaging channels with the laser tracking channel and parallel data fusion allows for improved identification of the target signatures.

Here we discuss the initial development and test results of a prototype AIMS with self-steering ALTS for TPD operations [1, 2]. When fully developed and implemented, this system should be capable of monitoring the 9D state vector of a remote, fast moving, and maneuvering target or cluster of targets, as well as assessing characteristics of the target's vibrational spectrum. The proposed active laser tracking approach uses optical phase conjugation (OPC) to enhance tracking accuracy and pointing stability [14], generate a weak signal amplification [15], and allow for correction of the atmospheric distortion [16], the latter two being critical problems in coherent optical imaging of remote objects. Unlike adaptive optic (AO) and software-based post-processing techniques (such as speckle imaging and blind deconvolution [17]), OPC operates inherently at an extremely high speed; this advantage is especially crucial for high-angular velocity objects such as those in the low earth orbit (LEO). Image-based active laser tracking

has also been demonstrated previously for boost-phase ballistic missile tracking with adaptive optic correction [18], and an OPC-enabled imaging/tracking technology could simultaneously address both the tracking and discrimination problems.

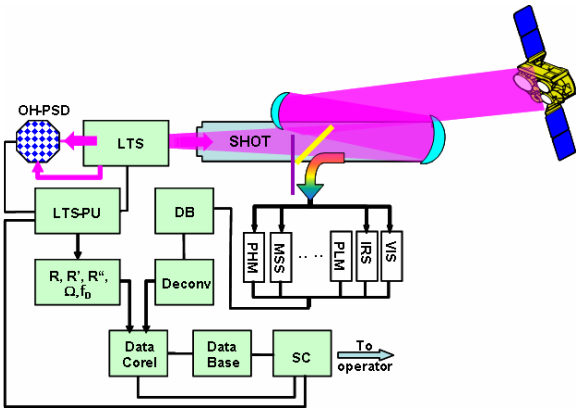

Fig. 1. Schematic diagram of the AIMS.

It is important, too, that this technology, when fully developed and deployed, will support not only space object tracking, but will also enhance identification and discrimination capabilities by retrieving the specific features associated with the vibrational spectrum and thermal distribution of the target. Last, but not least, the proposed technology may serve to improve free-space communication between ground-space and space-space platforms due to the stability in locking of the laser beam onto the remote target, a feature that is inherent to the proposed concept. Thus, the proposed technology has a clear potential for fusing separate components of TPD in a single instrumental design, moving the idea of the integrated TPD concept into a technical reality.

3. SYSTEM PERFORMANCE AND METRICS

There are several critical issues in AIMS architecture and operation requirements that define its performance. The following we would consider most critical and necessitate for an analysis: the system sensitivity required for shared optical train and multiple modules efficient performance, the resolution and energy budget for detecting and measuring essential target's parameters, including 3D state vector, velocity, vibration spectra, incoherent and IR imaging, and others. For proper estimation of these metrics it is essential to operate within a well defined range of parameters and with the high accuracy in each sensor category. This type of data for a number of candidate sensors is shown in **Table 1**.

Table 1. Expected accuracies for sensor modalities.

SYSTEM			DETECTION			TRACKING	IMAGING (SOI)	
Radar			Range (Single Pulse) (km)	Beamwidth / Cross Range Resolution	Down Range Resolution (m)	Varying Range (pulse integration) (km)	Cross Range ISAR (cm)	Down Range (cm)
Band	Size (m)	Signal Band-width MHz / %						
L/S	10	1 / 0.05	350	1 deg / 1.7 km @1000 km alt	150	1000	10	30 Spot ISAR
		20 / 1	170		7.5	460		
X	15	1 / 0.001	3500	0.12 deg / 0.2km@1000 km alt	30	8200	3	30 Stretched Pulse
		500 / 5	650		0.3	1750		
Laser Tracking			2000	<1 urad / 0.1-0.03 m	<0.01	2000	3-10.	< 0.1
Multi-Spectral Imaging			2000	Variable / N/A	N/A	2000	30	N/A

As an example, the combined use of accurate ranging data from ALTS and an imaging (or IR) sensor can lead to accurate target track position estimates, reducing the associated data uncertainty. However, the problem of initially combining ALTS and imaging data into a target track when the IR data have no range information is difficult. This

difficulty may be further compounded by the resolution differences of IR and ALTS or imaging sensors. This is a classical data fusion problem that must be addressed in this program.

3.1 Performance Metrics

Since the goal of AIMS is to integrate several sensors on a single operational platform, and explore the synergy among the metrics for all these sensors. Although the operational characteristics of these sensors are different, they can be divided into two categories, i.e., coherent for laser-based techniques and incoherent for others. The key parameter for any sensor operation is the signal-to-noise ratio (SNR) that defines AIMS resolution and its ultimate assessment capability for critical target features that lead to identification and characterization. The SNR for most of the detectors is a multi-variables parameter given by:

$$SNR_{IC} = \frac{\eta_D P_{SIG}^2}{2hfB\left[P_{BK} + P_{SIG}\right] + K_1 P_{DK} + K_2 P_{TH}} \quad (1)$$

where η_D is sensor quantum efficiency, P_{SIG} is received signal power, h is Planck's constant, $K_{1,2}$ are the coefficients that define detector's responsivity and dark current noise (1) and thermal noise (2), P_{DK} and P_{TH} is sensors equivalent dark current and thermal noise power, respectively; and P_{BK} is the background power, B is the electronic bandwidth. The SNR for a coherent detector can be expressed as:

$$SNR_C = \frac{E_T \sigma D^4 \eta_{sys} \eta_{atm}}{16 \lambda R^4 hc} \ , \quad (2)$$

where E_T is the transmitted laser power level, σ is the effective target cross-section, η_{atm} and η_{sys} are the atmospheric and system transmission factors, D is receiving aperture diameter, R is the system range to target.

In addition to the typical set of parameters, each detector has its specific metrics factor. For example, most of the commercially available uncooled IR sensors operate in the 8 to 12 μm range. Their performance is a function of sensitivity, resolution, and range. Sensitivity, the ability to resolve two objects of nearly equal apparent temperature, is measured by noise-equivalent temperature difference (NEdT) and minimum-resolvable temperature difference. NEdT, measured in mK, consists of the amount of IR radiation needed to produce a signal equal to the heat (noise) created by the detector itself. The lower the noise floor of the system, the lower the NEdT and the smaller the detectible signal. Ranging capability depends on resolution and sensitivity, often measured by the Johnson Criteria—the number of pixels required for users to detect the presence of an object; recognize it well enough to classify it; and identify it as a specific member of a class, such as a reentry vehicle versus a decoy.

3.2. Amplification of a Weak Signal with ALTS

For the ALTS to efficiently amplify the low intensity input signal, it is essential to estimate its sensitivity and the required energy of the pumping beams. For ALTS, the spontaneous Brillouin scattering is the ultimate source of noise for an angular element of resolution and is determined by scattering of the pump beams on thermal phonons:

$$W_N^{/} = \hbar\omega \times \bar{n} \times \Delta f \times \tau \ , \quad (3)$$

where $\hbar\omega$ is the photon energy, $\bar{n} = kT/\hbar\Omega \ \sim 10^3 - 10^4$ is the number of the thermal phonons at hyper sound frequency Ω_B that is equal to SBS shift in the NLM at temperature T, Δf is the frequency bandwidth of the gain of SBS FWM, and τ is the pulse duration of the scattered beam. As a result, the sensitivity of the PCM, for minimal energy of the signal beam in a signal spatial mode (on one element of the resolution), is:

$$W_{\min} = W_N^{'} \Big/ \eta \ , \quad (4)$$

where η is the quantum efficiency of the amplifier. For $\lambda = 1.06$ μm, and typical for $\Omega = 2\times10^{10}$ rad/s one can get:

$$W_{\min}\ [J] = 5\times10^{-16}\ \Delta f \times \tau\ /\eta. \quad (5)$$

The magnitude of $\Delta f \times \tau / \eta$ depends upon the character of the FWM. In the region of convective instability, SBS (the magnitude of η can be close to 1) the dimensionless bandwidth $\Delta f \times \tau$ is determined by duration of the pump beams and SBS bandwidth. In the region of the absolute instability of the SBS, the following ratio is correct: $\Delta f \times \tau \sim 1$. The value of η is defined as $\eta < 1$ if the duration of the pumping and signal beams is equal. For rectangular pulses of equal length, and in the absence of saturation effects the ratio $1/\eta \cong G/4$, where G = 25, is the total increment SBS in the field of the counter propagating waves. As a result, the sensitivity of the PCM is:

$$W_{\min} = 3\times10^{-15}\ \text{J}. \quad (6)$$

Equation (6**)** estimates a minimal energy per resolution element that can still be phase conjugated.

Next, we estimate the pump beam power required to operate the PCM. The regime of the absolute instability of the SBS can be achieved when the gain ($M = g \times P \times \ell / d^2$) exceeds the value of threshold $M_{th} \approx 8 - 12$, where g [cm/MW] is the coefficient of nonlinearity, P is the pumping beam power, d is its diameter, and ℓ is the optical path in the NLM. Thus, the pump beam power can be found from:

$$P \geq \frac{1}{2} P_{sig} \times \frac{d^2}{\lambda \times \ell} \sim \times \frac{\theta_B}{\theta_D}, \tag{7}$$

where θ_B is the divergence of a signal beam and θ_D is the diffraction-limited beam of the diameter *d;* and $P_{Sing} = \frac{25 \times \lambda}{2\pi \times g}$ is the SBS threshold power for a single-mode beam focused in the NLM with high nonlinearity. Thus, for $g = 2 \times 10^{-2}$ cm/MW, $P_{Sing} \approx 2 \times 10^{-2}$ MW, i.e., in order to resolve 100 spatial elements, the required pumping power should be about 2 MW, resulting in the energy level of 100 mJ per beam at pulse duration 50 ns; an energy that is fairly achievable in a laser system.

3.3. Range-Energetic Estimations for a Long-Range ALTS

To aid in understanding the system performance, we will now plot the beam energy at successive locations along the beam path. Round-trip losses differ significantly as system-operating parameters are varied with range distances from 0.5 to 10 km, aperture sizes up to 10 cm, and C_n^2 ranging from 10^{-16} to 10^{-13} $m^{-2/3}$. In an example at 10 km used to calculate the required system gain, we found that the round-trip losses without phase conjugation total ~ 90 dB.

The divergence of the outgoing beam was deliberately made large (0.1^o) for illumination of the whole target. The energy fraction impinging upon the aperture can be calculated by geometry. The solid angle subtended by the retroreflector with an aperture diameter D_{retro} is simply $(\pi/4)(D_{retro}/R)^2$, where R is the range; whereas the solid angle subtended by the beam is $(\pi/4)\theta_{FOV}^2$, where θ_{FOV} is the full-angle divergence of the illuminator beam (0.1^o in our case). The energy fraction intercepted is then simply the ratio of the solid angles, or $(D_{retro}/R\theta_{FOV})^2$. This equation strictly applies only if the beam is uniform, which was nearly the case for us. When atmospheric scintillation is present, the equation still applies over an average of many shots, but only when the target is not closer to the edge of the field of view than the spreading caused by atmospheric turbulence.

Atmosphere-induced beam spreading, of course, occurs for both the retro-reflected beams and the phase-conjugate beams. Its extent, particularly in the case of the phase-conjugated beam, can be calculated with beam-propagation computer programs. However, one can achieve more insight into the effects of atmosphere-induced beam spreading by using the physics of atmospheric turbulence to estimate the spreading. First, the theory defines a scale size, the transverse coherence length, for atmospheric turbulence. For horizontal propagation through homogeneous turbulence, this transverse coherence length is [19]:

$$r_0 = 1.44\left(C_n^2 k^2 R\right)^{-3/5}, \tag{8}$$

where C_n^2 is the strength of the turbulence, $k = 2\pi/\lambda$ is the wave number, λ is the optical wavelength, and R is the range. Second, a generally acknowledged empirical postulate is that the divergence of the entire beam (of diameter D) will be equal to the diffraction spreading of a beam having size $r_0 << D$. In this approximation, the beam spreading due to turbulence is, therefore, $\theta_{turb} \approx \lambda / r_0$. Finally, the fraction of energy captured by the system aperture of diameter D_{sys} is then the ratio of the solid angles, $(D_{sys}/R\theta_{turb})^2$, which has a $1/R^2$ dependence. For worst-case scenario of $C_n^2 = 10^{-13}$ $m^{-2/3}$ and R = 10 km, and with λ = 1064 nm, Eq. (8) yields $r_0 \approx 2.7$ mm, and the beam-spreading loss for a 10-cm transceiver aperture is ~ 23 dB. For a weakly turbulent atmosphere $C_n^2 = 10^{-16}$ $m^{-2/3}$ and the same distance, r_0 is equal to 17 cm. In this case, transverse coherent length exceeds the transceiver aperture, i.e., the atmospheric effect introduces less loss than diffraction beam spreading.

It follows from preliminary estimations that the total losses can reach up to 88 dB, while FWM technique allows a gain up to 60 dB (or 10^6). Since we project using laser heads with the amplification as much as 100X/pass the amplification at a level ¥ 30 dB is achievable.

Obviously, the above discussed metrics are not a complete list of all needed, but just give an indication of the complexity of the problems, and they will be extended as the work on this project progresses further.

4. AIMS DEPLOYMENT AND FIELD-TESTING

Detailed description of the development, system installation and some of the experimental operations are given in [3]. According to the approved test-plan the AIMS was deployed at the Precision Impact Range Area (PIRA), Edwards AFB. The AIMS was track-loaded as shown in Fig. 2, and was operating in totally self contained mode. The 20 kW Baldor generator provided sufficient electrical power to support a single-shot operation of the ALTS with its controllers and chiller, computers and electronic modules, though it was insufficient for system's high repetition rate function. There were other factors that would complicate tests performance such as, lack of shielding in the lab-designed AIMS to prevent the permeation of very fine dust particles inherent to this field test environment. Absence of the air-conditioning in the track made it difficult to operate the system efficiently. All these and other factors will be taking into account for next field-test experiments.

The track with the AIMS was installed at the top of the hill that dominated the test area, with AIMS oriented towards the sight line along the direction of 34° 50′ N/117° 38′ W. Such orientation was dictated by the test safety requirements and convenience in repositioning the target along the adjacent roads. On the other hand the system orientation resulted in an operating environment with the gusty wind (reaching up to 37 ml/h) hitting almost along the same line of sight but in the opposite direction, i.e. from South-West to North-East. This resulted in a strong instability of the track with AIMS, thus adding another level of the complexity to this field-test experiments, making them immersed in the realistic environment.

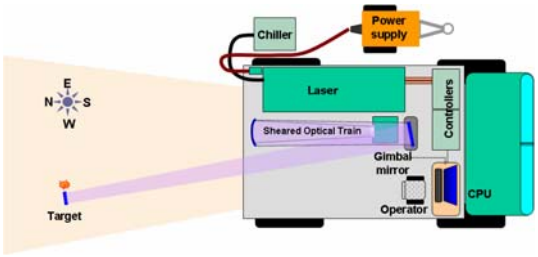

Fig. 2. Schematic of the track loaded AIMS

Once system was installed and adjustment were completed test was initiated starting with a shorter distance between the target and AIMS. Fig. 3 (a) illustrates the test area and the path of the vehicle with the target, starting from its nearest to the AIMS initial position. The white line on this figure shows the physical path of the target and the green line marks the direct line of sight to the most remote position of the target at about 6.38 km the system reliably detected and tracked. These data are complemented by the GPS-based records shown in Fig. 3(b) with distance to (blue line) and relative altitude (red line) at each tracked location. Position 7 on this figure represents the longest distance between the AIMS and the target and corresponds to about 6.4 km. Although further redeployment of the target along this line was still possible and ALTS system had possible enough capacity in performing tracking, however two critical factors that dictated test termination. Those two are local environment and topographical conditions. While topography on the ground restricted further movement area, numerous palm trees and bushes along the path made it very difficult to impossible to find a direct non-cluttered sight of view.

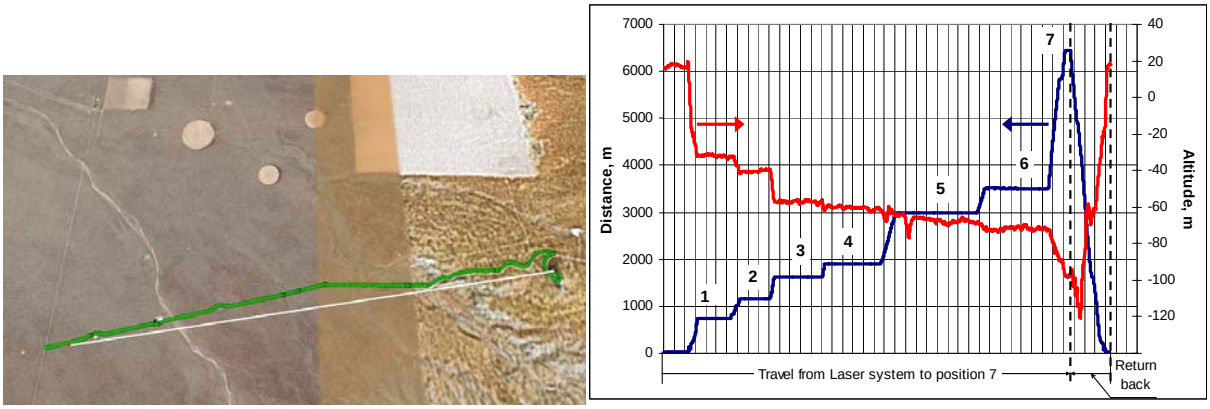

Fig. 3. Tracking zone (a) with marked path of the "target" vehicle (white line) and line of sight (green line), and distances and elevations for target spots (b) along the tracking path.

5. AIMS TEST RESULTS

The main purpose of the performed field-test and its results serve as a prove of the concept for:

- Joint operation of coherent (laser-based) and incoherent (visible and IR) multi-sensor system target detection through the shared optical train, and posterior data fusion for improved TPD operation;
- An active laser tracking through turbulent atmosphere layer with system operation based upon the principles of optical phase conjugation;
- Valid experimental demonstration of the laser system with a longest ever made mechanically unstable laser cavity;
- Retrieval of information on target's 3D state vector. In the current prototype design the system allows to detect the range and angular coordinate to the target, although an upgrade of the system capabilities (by incorporating a frequency agile local oscillator) will enable retrieval of target's velocity vector and its derivatives.

Although in a field test environment both coherent and incoherent operations and data have been received at once, here for simplicity of description we will present and discussed them separately.

5.1. Coherent detection - Active laser tracking.

In this section, we examine the capability of the system to be locked-on the target at different ranges and through turbulent atmospheric conditions. The sequence of images in Fig. 4 illustrates the lasing of the system as the targets moves step-by-step further along the path shown in Fig. 3, thus increasing the distance from the stationary AIMS platform. As it follows from Fig. 3 and 4 the longest distance we were able to achieve was 6.38 km. There was still enough power budget for further increase of the operational range, however rapid change in road topography (see a sharp slump of the red curve in Fig.3(b) around location 7) resulted in a loss of direct sight and effective coupling between the AIMS and the target.

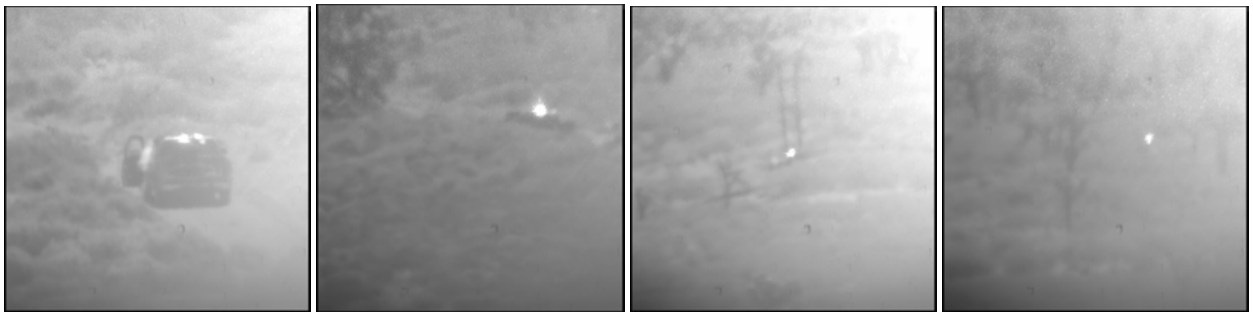

Loc. 2: 1.2 km **Loc. 3: 2.7 km** **Loc. 5: 3.6 km** **Loc.7: 6.38 km**

Fig. 4. Imaging of the lasing trace at different range between the laser tracking module and the target.

Side-to-side relative displacement of the target versus its locked position allowed to verify the system's field of view (FOV). The value of FOV was estimated previously at the laboratory conditions as $\theta_{FOV} \approx 0.017$ rad. The field test experiments and measurements supported very closely this value of θ_{FOV}. Indeed, stable oscillation and laser beam locking on the target has been observed within the θ_{FOV} angular zone. Any mutual tuning of the AIMS and the target outside of θ_{FOV} resulted in a sharp decline of the lasing energy and loss of locking on the target.

Experiments in coherent detection enabled also to perform measurements of the range between the AIMS platform and the target. This can be done through an analysis and comparison of the traces of oscillation in the local (master) and extended (slave) laser cavities. Since temporal behavior of these two traces of oscillation is coupled, what constitutes the operation of the coherent detection segment of the AIMS (detailed description of this segment is given in [3]), each representative pulse of the target-locked cavity has a corresponding pulse in the lasing trace of the master cavity (but not vice versa). By comparing these two traces enables to derive the range to the target, and two measuring methods can be applied in this case. It can be achieved by detecting the time delay between selected pulses in both channels or through analysis of the correlation between master and slave trace. Fig.5 illustrates typical result for a correlation function with measured distance 1.5 km (a round trip path difference and corresponding time delay are equal to 3.0 km).

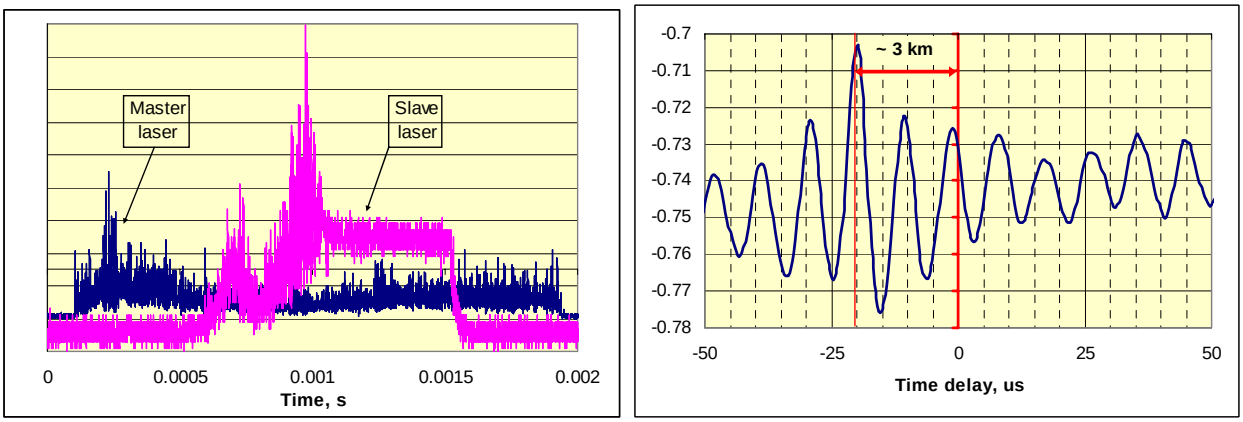

Fig. 5. Traces of oscillation for master and slave cavities (a) and their correlation function with derived time delay for a round trip.

Pulse relationship in both cases [18] provides comparable result as shown in Fig. 6. To some extend this latter technique is similar to laser burst method [20] with one significant distinction. Laser burst technique operates through the comparison of the outcoming and incoming (reflected off the target) sequence of pulses. This sequence of sent and returned pulses is totally independent, while in AIMS configuration those pulses are coherently coupled, and, therefore should allow the use of a higher level correlation or use of coherent detection technique, such as heterodyne.

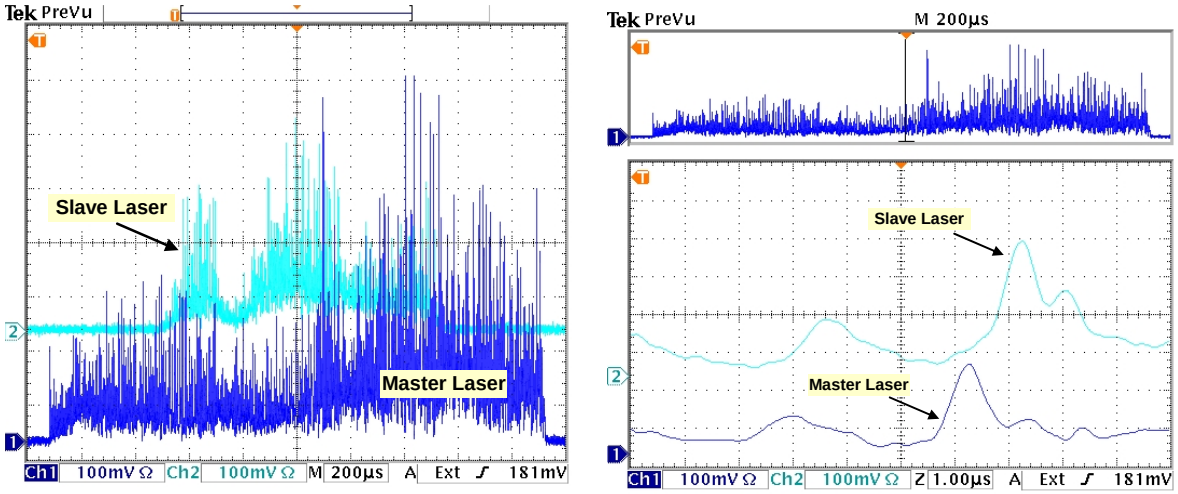

a) b)

Fig. 6. Lasing traces of the of Slave and Master cavities at ALTS-target distance 1.5 km.

5.2 Incoherent detection – passive multi-sensor suite

In the proposed system architecture shown in Fig. 1 set of incoherent detection can operate through a common optical train. The advantages of such a configuration have been already discussed in the preceding sections of this paper, and here we just present some technique used and results received.

Fusing multiple bands collected from dissimilar sources (and therefore having different "scaling" and "weight" functions in the imaging format) necessitates first for scaling and registering the various images to account for variations in camera orientation and resolution in the system. This can be achieved by using an affine transformation of the imagery, although the current technique could easily be extended to the use of an x-y homology technique if the need arose. The specific affine transformation routine used is the `Image.transform` function implanted in the Python Imaging Library. It employs a 2×3 matrix of the following form to resample in input image pixels to the output image pixels:

$$\begin{bmatrix} x_{in} \\ y_{in} \end{bmatrix} = \begin{bmatrix} a & b & c \\ d & e & f \end{bmatrix} \cdot \begin{bmatrix} x_{out} \\ y_{out} \\ 1 \end{bmatrix} \tag{9}$$

This is used in conjunction with a bicubic interpolation filter to interpolate the transformed image. The closed form solution of the optimal linear transformation as described in [21] was applied here in order to establish the necessary values for the affine transformation matrix. Given a set of *n* manually obtained correspondence points in the input image $\vec{r}_{r,i} = \begin{bmatrix} x_{in,i} \\ y_{in,i} \end{bmatrix}$, and the corresponding set of points in the output image: $\vec{r}_{l,i} = \begin{bmatrix} x_{out,i} \\ y_{out,i} \end{bmatrix}$

By using this technique we were to fuse data from two sources with complementary information and get a single-shot image that incorporates multiple values in a color coded format as shown in Fig. 7 (b). Certainly this technique requires for further improvement and enhancement, however we must admit that to the best of our knowledge this is the first time when the images with coherent and incoherent emission (of very different spectral bands) zones on the target have been put together for its potentially better perception and identification.

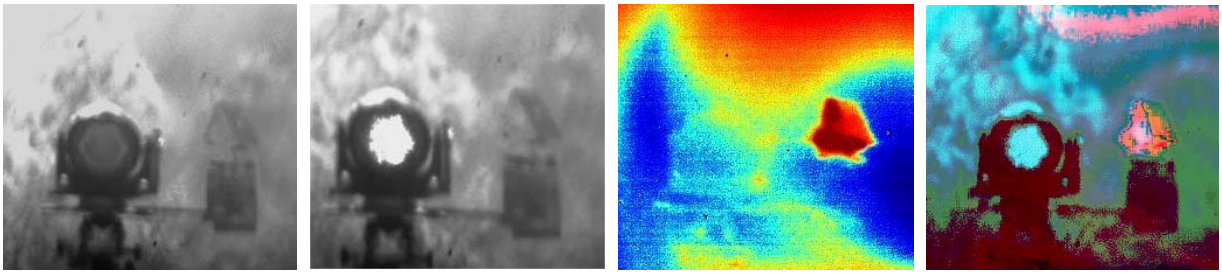

Fig. 7. Visible image of a target set without (a) and with (b) lasing spot taken by CCD camera, IR image of the target (c) and fused image received from integration of images.

5.3 Follow-on tests

Next steps in spiral development of the AIMS capabilities should comprise of:

- Tracking operation along ground-to-air line of sight.
- Validation of the AIMS working envelop, in particular:
  - Factors limiting the operational range and performance of the laser tracking module and their augmentation;
  - Demonstration of capabilities in measuring the target's 3D state vector and its derivatives;
  - Enhancement of AIMS capabilities through broadening its operational spectral band and functionality of incoherent detectors (LWIR, colorimetric, polarimetric, others).
- Synchronization and fusion of the data with different modalities, i.e: imaging (from different spectral bands), non-imaging (3D state vector and it derivatives);
- System operation at image-resolved and nor-resolved conditions (i.e. short-range versus long-range) [22];

Augmentation of AIMS capabilities and improvement in its performance for stepwise progress from a high-altitude aircraft, to LEO and MEO satellites and beyond can be achieved through the following steps:

- Gradual increase of the lasing budget. Current prototype AIMS design is to demonstrate basic functionality of its principles of operation. The follow up tests will be directed towards high-altitude aircraft, although the system capabilities will not allow to get the outer space targets, limited by budgeting constrains;
- An optimized design of the shared optical train, aimed to reduce the losses for passive and active tracking sensors;
- Integration of a high speed, programmable tunable local oscillator, needed to retrieve the derivatives of the 3D state vector (i.e. velocity, acceleration) as the indicators of target maneuvering;
- Incorporation of nonlinear optical coherent receiver with amplification and phase conjugation of the emission scattered by non-cooperative target with the level of detection of the order of a few tens of photons on the resolved spatial mode. This will enable for a high-confidence detection and discrimination of the remote target.

6. CONCLUSION

This paper discusses the progress in the development and field-testing of an advanced integrated multi-sensor system (AIMS) for an enhanced space surveillance capability. The field-testing of a prototype AIMS validated the feasibility of AIMS concept for potential application to space superiority, ISR, JWS and homeland defense mission areas. The key AIMS innovation is to integrate various active and passive sensors on a single platform, all of them operating through a shared optical train. Such architecture enables for simultaneous data flow from the sensors with different capabilities and metrics, real-time synchronization of sensing data, and their concurrent fusion. Thus results in an increased reliability in target detection, tracking and discrimination. An advanced approach based on OPC principles used in the design of the active laser tracking module applied in AIMS allows system operation through a strong atmospheric turbulence, thus paves the foundation for an effective ground based space surveillance system. The AIMS filed-test, first in a series to be performed in a realistic operational environment, substantiated the functionality of the unique approach, its sustainable performance and reliable data retrieval. Experimental data collected and lessons learned will be used to design and size the next level of AIMS prototype with significantly extended operating range, and the selection and design of test equipment to support a much less constrained testing environment.

ACKNOWLEDGEMENTS

This research was sponsored by the United States Air Force, Space and Missile Systems Center, SMC/XD at Los Angeles AFB and Air Force Research Laboratory AFRL/VSSE at Kirtland AFB under the Contract No. FA9453-05-C-0031. Any opinions, findings and conclusions or recommendations expressed in this material are those of the author(s) and do not necessarily reflect the view of the AFRL/VSSA and SMC/XD.

REFERENCES

1 V. Markov, A. Khizhnyak, E. Scott, B. Zel'dovich, T. Martinez, S. Liu, System Concept and some Characteristics of the Coupled-Cavity Laser System for Active Target Tracking, Proc. SPIE, Vol.4825, pp. 89- 98, 2002

2 V. Markov, A. Khizhnyak, Adaptive Laser System for Active Remote Object Tracking, Proc. IEEE Aerospace Conference-2002, (Big Sky, MT) 2002.

3 V. Markov, A. Khizhnyak, D. Wall, S. Liu, Field-Testing of an Active Laser Tracking System (ALTS), 2006 AMOS Technical Conference.

4. K. Kim Luu, Charles L. Matson, Capt Joshua Snodgrass, S. Maile Giffin, Kris Hamada, John V. Lambert, Object Characterization from Spectral Data, 2003 AMOS Technical Conference. Maui, HI. September 2003.

5 J.A. Ratches, R.H. Volmerhaususen, R.G Driggers. Target acquisition performance modeling of infrared system, IEEE Sensors J., Vol. 1, 31-40, 2001.

6 D. Hall, et al. AEOS I-Band Photometry of Moving Targets. 2003 AMOS Technical Conference. Maui, HI, 2003.

7 Bush, K.A., Crockett, G.A., et al., Satellite Discrimination From Active and Passive Polarization Signatures: Simulation Predictions Using the TASAT Satellite Model, Proce. SPIE, Vol. 4481, 46-57, 2002

8. Civilian Satellite Remote Sensing: AStrategic Approach, OTA-ISS-607, 1994

9 M.R. Pearlman, J.J. Degnan, and J.M. Bosworth, The International Laser Ranging Service, Advances in Space Research, Vol. 30, 135-143, 2002.

10 Jorgensen, K., Okada, J., Bradford, L., Hall, D., Africano, J., et all, Obtaining Material type of Orbiting Objects through Reflectance Spectroscopy Measurements. AMOS Proc. 2003.

11. J.Llinas, D.L. Hall, An introduction to Multi-Sensor Data Fusion, Proc. IEEE International Symposium on Circuits and Systems, 537-540, 1998.

12. L. Klein, *Sensor and Data Fusion*, SPIE Press, Billingham, 2004

13. R. Sobek, C.Malone, Time Optimal Strategy for Target Acquisition Handoffs, SPIE Proc., Vol. 4265, 1-9, 2001.

14. V. Markov, A. Khizhnyak, S. Liu, T. Martinez, Long-Range Adaptive Laser Tracking System (ALTS): Operational Principles, Concept Design and Potential Applications. AMOS Proc. 2003.

15. V.Wang, C. Guliano, Correction of Phase Aberrations via Stimulated Brillouin Scattering, Opt. Lett. 2, 4–6, 1978.

16. G. Gebur, E. Wolf, Phase Conjugation with Random Fields and Deterministic and Random Scatterers. Optics Lett. Vol. 24, pp. 10-12, 1999.

17. S.M. Jeffries, K.J. Schulze, C.L. Matson, S.M. Giffin and J.M. Okada, Blind Deconvolution with use of a Phase Constraint, AMOS Technical Conference, Kihei HI, 2002.

18. P. Merritt, S. Cusumano, M. Kramer, S. O'Keefe, and C. Higgs, Active Tracking of a Ballistic Missile in the Boost Phase, Proc. SPIE 2739, pp. 19-29, 1996.

19. G.C. Valley, Long-and Short-Term Strehl Ratios for Turbulence with Finite Inner and Outer Scales," Appl. Opt.,Vol 18, pp. 984-987, 1979.
20. M.R. Pearlman, J.J. Degnan, and J.M. Bosworth, The International Laser Ranging Service, Advances in Space Research, Vol. 30, 135-143, 2002.
21 B. Horn, H. Hilden, and S. Negahdaripour. *Closed-form solution of absolute orientation using orthonormal matrices*. J. Opt. Soc. Am. A, Vol. 5, p. 1127--1135, 1988.
22. M.Vorontsov, V. Kolosov, " Target-in-the-loop beam control: basic considerations for analysis and wave-front sensing", J. Opt. Soc. Am. A, Vol. 22, No. 1, pp. 126-140, 2005.